Vacancies and interstitials in indium nitride: Vacancy clustering and molecular bondlike formation from first principles

X. M. Duan and C. Stampfl
School of Physics, The University of Sydney, Sydney, New South Wales 2006, Australia
(Received 5 March 2009; published 8 May 2009)

We investigate the structural and electronic properties and formation energies of vacancy, interstitial, and antisite defects, as well as complex formation, in wurtzite InN using first-principles calculations. The N interstitial, which forms a split-interstitial configuration with a N_2-like bonding, has the lowest formation energy under N-rich conditions in *p*-type material, where it is a triple donor. We find that indium vacancies have a tendency to form "clusters," which results in local nitrogen-rich regions and the formation of N_x-molecular-like bonds. These complexes are amphoteric, have a relatively high formation energy, and are formed more readily under N-rich conditions. The nitrogen vacancy is a low energy defect under more In-rich conditions, and in *p*-type material it acts as a single and triple donor. In the neutral and negative charge states, we find nitrogen vacancies also prefer to be situated close to one another and to cluster, giving rise to local In-rich regions with electron localization at these metalliclike bonding configurations. The indium antisite in the 4+ charge state is the lowest-energy defect under In-rich conditions in *p*-type material and thus also acts as a donor. Our findings shed light on, and help explain, recent and sometimes conflicting, experimental observations.

DOI: 10.1103/PhysRevB.79.174202 PACS number(s): 71.15.Nc, 71.55.−i, 71.15.Mb

I. INTRODUCTION

The group III nitrides (GaN, AlN, and InN) have attracted growing technical and scientific interest due to their applications in, e.g., short-wavelength optoelectronic devices, such as light-emitting diodes and lasers.[1–3] Indium nitride is also of interest in relation to other technological applications such as solar cells and optical wave guides.[4,5] Moreover, recent studies show that InN and other III nitrides are promising materials for high-speed electronics and terahertz devices.[6,7] Compared to GaN and AlN, the physical properties of InN (Refs. 8 and 9) are much less well established, largely due to the difficulties in synthesizing high quality single crystals. Only recently these problem have been overcome,[10] but key parameters still have not been conclusively determined. For example, a controversial issue is the value of the band gap: it has been long accepted as 1.9 eV but more recent experiments[11,12] and first-principles calculations[13–17] support a significantly lower value of around 0.7–0.8 eV, although some recent experiments[18] reported a somewhat larger value of 1.4 eV. The discrepancies in earlier reported band gaps (which range from ~0.65 to ~2.3 eV) may be due to poor material quality, i.e., nonstoichiometries, defects, and impurities,[19–22] which could form more readily due to the low thermal stability of InN.[23] Grown InN films are highly *n* type, which has been attributed to impurities (O_N and Si_{In}) (Ref. 24) and native point defects (the nitrogen vacancy).[25,26]

For the advancement of technological applications that utilize InN, it is important to have a deeper understanding of the behavior, role, and effect that defects and their complexes have on the atomic and electronic structure. Such knowledge is crucial to control the material properties and, ultimately, the device characteristics. There has been a first-principles investigation of point defects and impurities (O, Si, and Mg) in zinc blende (zb) InN (Ref. 24) using density-functional theory (DFT) and the local density approximation (LDA), as well as including self-consistent self-interaction (and relaxation) corrections. This study found that the N vacancy is the lowest-energy native defect and that it is a donor in more *p*-type material. The Si and O impurities are very low energy defects and are also donors, possibly contributing to the high *n*-type background in grown material. The In vacancy and the Mg dopant were found to be triple and single acceptors, respectively. But due to the smaller band gap of InN compared to GaN and AlN, unlike the latter two compounds, these two defects remain relatively high in energy in InN.

In the present paper, we investigate the atomic and electronic properties, as well as associated formation energies, of native point defects and complexes in wz InN through *ab initio* calculations. We identify a number of interesting phenomena: first, "surprisingly," we find that the indium vacancies and nitrogen interstitial introduce magnetism, where the value of the spin depends on the charge states. Second, we find that indium vacancies have a tendency to form "clusters" resulting in the formation of N_x-molecular-like bonds, and third the N interstitial results in the formation of a N_2-like-molecular bond ("N-split-interstitial") configuration and has the lowest formation energy in the 3+ charge state under N-rich conditions in *p*-type material. Finally, the indium antisite, in the 4+ charge state, is the lowest-energy defect under In-rich conditions and in *p*-type material. As reported in detail elsewhere,[27] we also found that the N vacancies in the neutral and negative charge states prefer to be located close to one another, (i.e., to "cluster together"), giving rise to a locally In-rich region. All these findings shed significant light on the behavior of native defects and complexes in indium nitride. The paper is organized as follows: in Sec. II, we describe the calculation method, and Sec. III reports results for native defects and their complexes. Sec. IV contains a discussion of our findings in light of experimental results, and Sec. V contains the conclusions.

II. CALCULATION METHOD

Our DFT calculations are performed using the LDA for the exchange-correlation functional, as well as the pseudopotential plane-wave method in a supercell geometry, with the ESPRESSO code.[28] We treat the indium 4*d* electrons with the nonlinear core correction (nlcc) (Ref. 29) and include scalar-relativistic corrections. The energy cutoff is 60 Ry, and we use 96 atom wz supercells, where all the atoms are fully relaxed. A reciprocal space **k**-point mesh of $3\times3\times3$ is used. Further details of the method and convergence tests can be found in Ref. 27.

The formation energy of the defect system (e.g., a nitrogen vacancy, V_N) in the charge state q is given by

$$E^f(V_N^q) = E^{tot}(V_N^q) - E^{tot}_{bulk} + \mu_N + q(E_F + E_v + \Delta V), \quad (1)$$

where $E^{tot}(V_N^q)$ is the total energy of the supercell containing the vacancy in charge state q and E^{tot}_{bulk} is the total energy of a supercell of the same size, containing only bulk material. μ_N is the chemical potential of the nitrogen atom and E_F is the Fermi level, which is chosen to be zero at the valence-band maximum (VBM) (E_v) of bulk InN. A correction term ΔV is added to align the reference potential in the defect supercell with that in the bulk.[30] From examination of the associated defect induced states of the neutral system, the relevant charged states to be investigated are identified. We consider N-rich and In-rich conditions, where for the former, $\mu_N = 1/2\mu_{N_2}$ (which here corresponds to half the total energy of the N_2 molecule) and μ_{In} is determined by assuming thermodynamic equilibrium: $\mu_{In}+\mu_N=\mu_{InN}$, where μ_{InN} is the chemical potential of bulk InN (which corresponds to the total energy of a bulk InN stoichiometric unit). For In-rich conditions, $\mu_{In}=\mu_{In}$ (bulk) (i.e., the total energy of an In atom in the bulk In metal), and μ_N is determined by the assumed condition of thermodynamic equilibrium given above. The formation energy then allows us to determine the lowest-energy defect, that is, which defect configuration is most likely to exist in InN under certain experimental conditions (e.g., nitrogen-rich or indium-rich; *p*-type or *n*-type).

Since in the present paper, we also investigate complex formation, it is useful to consider the "binding energy" of the various complexes. The binding energy of a complex (e.g., two vacancies V_N+V_{In}) in the charge state q is defined with respect to the separated defects,

$$E_b[(V_N + V_{In})^q] = E^f[V_N^{q_1}] + E^f[V_{In}^{q_2}] - E^f[(V_N + V_{In})^q], \quad (2)$$

where $q=q_1+q_2$, $E^f[V_N^{q_1}]$, and $E^f[V_{In}^{q_2}]$ are the formation energies of the defect V_N in the charge state q_1 and the defect V_{In} in the charge state q_2, respectively. The sign of E_b is chosen such that a positive binding energy corresponds to a bound complex.

III. RESULTS

The optimized wurtzite InN lattice constants are $a=3.511$ Å, $c/a=1.624$, and $u=0.376$, which agree very well with the experimental values (3.533, 1.611, and 0.375 Å).[31]

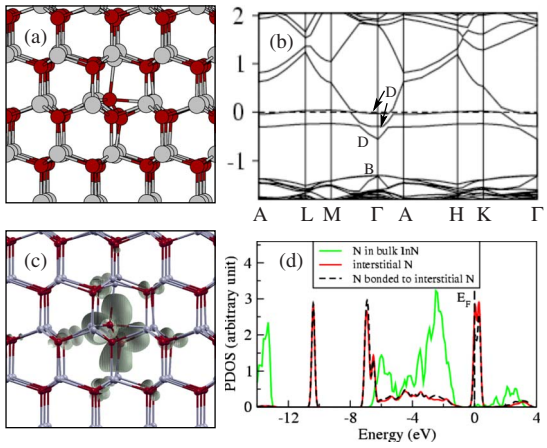

FIG. 1. (Color online) (a) Atomic geometry and (b) band structure of the *T*-site nitrogen split interstitial in the neutral charge state. (c) The isosurface of the electron density of the lower defect induced state marked by the arrow in (b). Partial density of states (PDOS) of the N interstitial (d) in the neutral charge state. Labels "B" and D in (b) indicate bulk and defect states, respectively. The horizontally dotted line in (b) indicates the Fermi level.

The calculated heat of formation is −1.16 eV, which is in line with the experimental values which range from −0.22 to −1.49 eV.[31] The cohesive energy of bulk In in a body-centered tetragonal structure is calculated to be −3.52 eV with the lattice parameters $a=3.011$ Å and $c=4.756$ Å. Here we used a $6\times6\times6$ **k**-point mesh and an energy cutoff 60 Ry. From all-electron *ab initio* LDA calculations[32] the cohesive energy is −3.25 eV (with the lattice constants $a=3.20$ Å and $c=4.905$ Å) and the experimental value is −2.52 eV (Ref. 33) [$a=3.24$ Å and $c=4.937$ Å (Ref. 34)]. Spin-unrestricted calculations are performed to study the nitrogen atom and molecule. The binding energy of N_2 is calculated to be 5.56 eV/N atom, while the bond length is 1.103 Å. From experiments, the corresponding values are 4.96 eV/N atom and 1.098 Å.[35] The LDA is known to overestimate the cohesive energy and the binding energy, and the nlcc approach underestimates lattice parameters (in particular for bulk In) and overestimates somewhat the cohesive energy and heat of formation, as has been reported in Ref. 36. These results are discussed in more detail in our earlier publication.[27]

A. N interstitial

For the single nitrogen interstitial (N_i) in wz InN, there are two types of high-symmetry positions: the (tetrahedral) *T* and (octahedral) *O* sites. The *T* site has two nearest neighbors (one cation and one anion) and six next-nearest neighbors (three cations and three anions). The *O* site has six nearest neighbors (three cations and three anions). We find that for both sites, after full atomic relaxation, a split-interstitial configuration creates in which N_i forms a N-N bond with one of the neighboring nitrogen host atoms, sharing its lattice site [see Fig. 1(a)]. The *T* site is lower in energy than the *O* site by 0.13 eV; thus, we focus on the *T* site for calculation of the charge states. This defect induces a

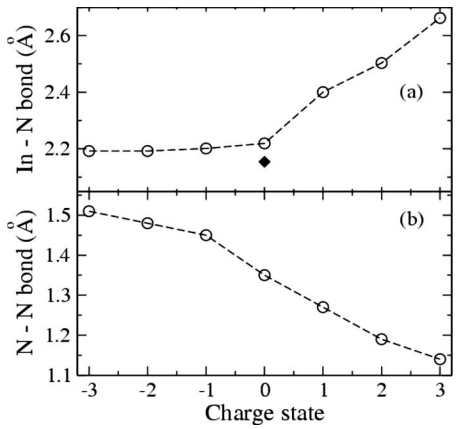

FIG. 2. Bond distances in the T-site N_i split-interstitial defect as a function of charge state. (a) The average bond length between the "N_2 dimer" configuration and the surrounding four In atoms. The filled diamond indicates the In-N bond distance in the bulk. (b) The N-N bond distance in the split interstitial. Circles represent calculated values; dashed lines serve as a guide to the eyes.

doubly occupied singlet defect state, a singly occupied singlet state, and an unoccupied defect state in the conduction band as shown in Fig. 1(b). Therefore we consider charge states from 3− to 3+. In Fig. 1(c) the square of the wave function is shown for the singly occupied defect state above the conduction-band minimum (CBM) indicated by the lower arrow in the band structure [Fig. 1(b)]. It can be seen that the defect state is localized at N_i and its nearest-neighbor N atom. The formation of the N_2-like bonding is also indicated by the PDOS shown in Fig. 1(d). It is clearly seen that the two N atoms involved in the N-split interstitial are quite different from the bulk N atoms, where they induce additional peaks both in the valence band and in the conduction band.

The interstitial N_i and its nearest-neighboring N atom relax significantly depending on charge state: in the neutral state [as shown in the Fig. 1(a)], the N-N distance is 1.35 Å. Removing one electron to create the 1+ charge state results in the N-N bond distance decreasing to 1.275 Å. In the 2+ and 3+ charge states, the distances are further reduced, namely, to 1.19 and 1.14 Å, respectively. The bond distance of 1.14 Å is very close to that of the N_2 molecule (1.10 Å). Adding electrons to create minus charge states results in the N-N bond length increasing to 1.45 Å in the 1− charge state and to 1.49 and 1.51 Å in the 2− and 3− charge states, respectively. Despite these changes, the split-interstitial configuration remains common to all charge states. The 3+, 1+, 0, and 1− charge states are stable where the formation energy of the 3+ charge state is very low under N-rich conditions in the p-type material. There are also corresponding changes in the N-In distances as shown in Fig. 2, where with increasing charge state, in particular, from 0 to 3+, the N-In distances increase. For the 3+ charge state, the surrounding In atoms exhibit large outward relaxations of ~23% relative to the bulk positions. A similar relaxation in the N-In bond lengths is found for V_N^{3+} in Ref. 27. This suggests that for the split interstitial in the 3+ charge state, the configuration could be viewed as V_N^{3+} plus a N_2 dimer "floating" in the void. In this configuration, the N-N pair does not strongly bond to the surrounding In atoms, and the average bond length between the interstitial N atoms and the surrounding In atoms is much larger than the bulk In-N bond length (see Fig. 2). As more electrons are added to the N_i^{3+} defect, the N-N bond becomes weaker (as indicated by the increased N-N distance) and the tendency to form bonds with the surrounding In atoms increases. A similar behavior has been found for the nitrogen split interstitial in AlN (Ref. 37) and GaN (Ref. 38): for the nitrogen split interstitial in zb AlN, the charge states from 3+ to 1− are considered and only the 3+, 1+, 0, and 1− charge states are stable,[37] i.e., the 2+ charge state is unstable as we found for wz InN. For the nitrogen split interstitial in wz GaN, charge states from 3+ to 3− were considered and the 3+, 2+, 1+, 0, and 1− charge states are stable.[38]

We perform spin-polarized calculations for the nitrogen split interstitial and find that it is magnetic in the neutral charge state: the total magnetization is $1.09\mu_B$, and the total energy of the spin-polarized state is 125 meV lower than that of the nonspin-polarized state. The magnetic moment is mainly localized on the $2p$ electrons of the interstitial nitrogen, which carries a magnetic moment of $0.49\mu_B$ and the bonded host nearest-neighboring N atom has a magnetic moment of $0.39\mu_B$. The nitrogen split interstitial is nonmagnetic in the 3+ charge state.

B. Antisites

We investigate two antisite configurations, namely, the N atom on an In site, N_{In}, and the In atom on a N site, In_N. The nitrogen antisite, N_{In}, induces three doubly occupied singlet defect states above the VBM, and three higher lying unoccupied defect states. Since the calculated formation energy in the neutral charge state is very high (6.25 eV under N-rich and 8.57 eV under In-rich conditions), we only consider the charge states from 2+ to 4− and find that the stable states are 1+, 0, 1−, (in a very narrow energy window) and 3−. Atomic relaxation results in a strong distortion, where the nitrogen atom on the In site moves toward a N neighbor and forms a N-N bond. We note that due to the strong relaxation, this defect could be described as a complex consisting of a N-split interstitial plus an In vacancy. The bond length changes with respect to the charge state: filling the defect levels decreases the bond length from 1.22 Å in the neutral charge state to 1.16 Å in the 3− charge state. The distance to the other three N neighbors is much larger (2.2 Å), indicating no bond is formed. Removing two electrons from the neutral N_{In} defect state results in bond formation between N_{In} and its three planar N neighbors, with an average planar bond length of 1.57 Å and an apical bond length of 1.52 Å. The behavior of the nitrogen antisite in GaN is somewhat different: it has been found from *ab initio* investigations that the nitrogen antisite in GaN is characterized only by a single N-N bond from 2+ to 4− charge states and no bond between N_{Ga} and its three planar N neighbors forms.[30] The formation energy of the nitrogen antisite, in all of its charge states and under both N-rich and In-rich conditions, is quite high (see Fig. 8); thus it is unlikely that N_{In} will form in appreciable concentrations in thermal equilibrium. However, their forma-

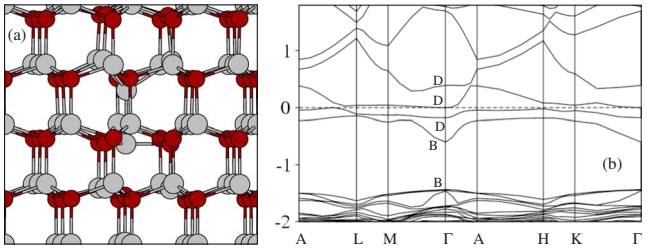

FIG. 3. (Color online) (a) Relaxed atomic geometry and (b) band structure of the antisite In_N in the neutral charge state. Dark and light spheres represent N and In atoms, respectively. Labels B and D in (b) represent bulk and defect states, respectively. The horizontally dotted line in (b) indicates the Fermi level.

tion may be induced under nonequilibrium conditions.

In the neutral charge state, the indium antisite, In_N, induces a doubly occupied singlet defect state and two unoccupied defect states above the CBM. In the DFT calculations, the CBM is also occupied by two electrons. In reality, however, these two electrons should be associated with the defect [see Fig. 3(b) which shows the band structure]. Thus the relevant charge state that we can consider is 4+. The calculated formation energy of In_N under N- and In-rich conditions is shown in Fig. 8: under N-rich conditions, the formation energy remains too high for it to occur in significant concentrations in thermal equilibrium, but under In-rich conditions this defect has the lowest formation energy in *p*-type material. In the antisite geometry, the substitutional In atom forms four bonds to the surrounding nearest-neighbor In atoms, with an average In-In bond length of 2.59 Å in the neutral charge state and 3.06 Å in the 4+ charge state. While the bond length in the neutral charge state is much shorter than the bond length in bulk In (3.25 Å), in the 4+ charge state it is only 5.8% smaller. From analysis of the electron localization function,[39] we find the dangling bonds between the In atom on the N site and its nearest-neighbor In atoms in the neutral charge state, are localized at the In antisite itself. The metallic character suggests that the indium antisite could be related to the observation of metallic states, in both MBE- and metal-organic chemical vapor deposition-grown InN by infrared photoluminescence measurement.[18]

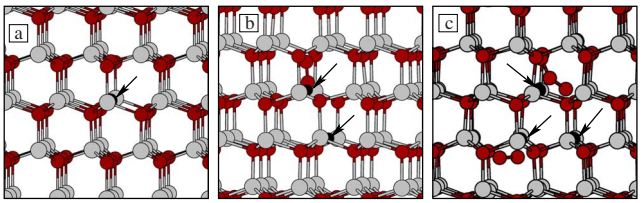

FIG. 4. (Color online) Relaxed atomic geometry in the neutral charge state for (a) one, (b) two, and (c) three indium vacancies for the most favorable configurations. Dark and light spheres represent N and In atoms, respectively, and small black spheres indicate the V_{In} sites, which are also indicated by arrows.

C. Vacancies

For the indium vacancy, V_{In}, in InN [see Fig. 4(a)], the nearest-neighbor nitrogen atoms relax about 7% outwards with respect to the bulk positions. In the neutral charge state, the indium vacancy induces states close to the VBM which can be filled with three electrons, thus acting as a triple acceptor. This behavior is similar to V_{In} in zb InN.[24] The calculated formation energy in the neutral charge state is very high (~7.78 eV N-rich and ~8.94 eV under In-rich conditions). By plotting the square of the wave function, we find that the defect states induced by the indium vacancy are localized on the nearest-neighbor N atoms. For the different negative charge states considered, from 1− to 3−, we find that the magnitude of the outward relaxation decreases with increasing electrons in the system (see Table I). In the 3− charge state, the nearest-neighbor "planar" (three equivalent) nitrogen atoms of the indium vacancy are then just slightly

TABLE I. Change in defect geometry with charge state (q) for the indium vacancy, nitrogen vacancy, and indium-nitrogen vacancy pair. Units are in percent with respect to the values for InN bulk. r_{planar} indicates distances from the ideal vacancy position to the three (two for the vacancy pair) equivalent neighbors, and r_{apical} is the distance to the remaining neighbor in the [0001] direction.

	V_N			V_{In}	
q	r_{apical}	r_{planar}	q	r_{apical}	r_{planar}
0	−3.02	−3.33	0	8.03	6.08
1+	−0.98	−2.08	1−	6.08	4.80
2+	10.03	4.14	2−	4.37	2.94
3+	33.16	18.54	3−	2.15	0.41
	V_N in V_N+V_{In}			V_{In} in V_N+V_{In}	
q	r_{apical}	r_{planar}	q	r_{apical}	r_{planar}
1+	40.5	17.5	1+	36.5	0.31
0	−6.83	−4.10	0	6.55	4.61
1−	−5.84	−8.30	1−	4.25	2.91
2−	−6.28	−8.20	2−	−0.18	−0.47

TABLE II. The binding energies, E_b, in eV, for the defect complexes in stable charge states. The binding energies of the defects are computed with respect to the defect combinations in the parentheses.

Defect	q		E_b/V_{In}	q		E_b/V_{In}	q		E_b/V_{In}
V_N+V_{In}	0	$(V_N^+ + V_{In}^-)$	2.16	1−	$(V_N^+ + V_{In}^{2-})$	2.48	1+	$(V_N^+ + V_{In}^0)$	2.24
	0	$(V_N^{3+} + V_{In}^{3-})$	3.82	2−	$(V_N^+ + V_{In}^{3-})$	2.77	1+	$(V_N^{3+} + V_{In}^{2-})$	3.0
V_N+N_{In}	0	$(V_N^+ + N_{In}^-)$	2.36	1+	$(V_N^+ + N_{In}^0)$	2.09	2+	$(V_N^+ + N_{In}^+)$	1.59
	0	$(V_N^{3+} + N_{In}^{3-})$	5.33	3+	$(V_N^{3+} + N_{In}^0)$	3.39	2+	$(V_N^{3+} + N_{In}^-)$	4.29
				2−	$(V_N^+ + N_{In}^{3-})$	2.35			
$2\ V_{In}$	0	$(V_{In}^0 + V_{In}^0)$	3.66	3−	$(V_{In}^- + V_{In}^{2-})$	2.48	6−	$(V_{In}^{3-} + V_{In}^{3-})$	−0.76
				3−	$(V_{In}^0 + V_{In}^{3-})$	3.40			
$3\ V_{In}$	0	$(V_{In}^0 + V_{In}^0 + V_{In}^0)$	9.84	3−	$(V_{In}^- + V_{In}^- + V_{In}^-)$	7.35	6−	$(V_{In}^{2-} + V_{In}^{2-} + V_{In}^{2-})$	1.86
	5−	$(V_{In}^0 + V_{In}^{2-} + V_{In}^{2-})$	3.78	3−	$(V_{In}^0 + V_{In}^- + V_{In}^{2-})$	7.80	6−	$(V_{In}^- + V_{In}^{2-} + V_{In}^{3-})$	2.28
	5−	$(V_{In}^- + V_{In}^- + V_{In}^{3-})$	4.26	3−	$(V_{In}^0 + V_{In}^0 + V_{In}^{3-})$	8.70	6−	$(V_{In}^0 + V_{In}^{3-} + V_{In}^{3-})$	3.21
	5−	$(V_{In}^0 + V_{In}^{2-} + V_{In}^{3-})$	4.68						

larger (0.41%) than the equilibrium In-N bond length, and the apical N atom 2.15% larger.

Recently, it has been reported that the Al vacancy in AlN leads to spin-polarized ground states.[40] We perform a spin-polarized calculation for V_{In} and find: the total magnetization is $3.0\mu_B$ for the neutral indium vacancy. For the singly negatively charged vacancy, V_{In}^{1-}, it has a total magnetic moment of $2.0\mu_B$ and the doubly negatively charged vacancy, V_{In}^{2-}, carries a magnetic moment of $1.06\mu_B$. The closed shell V_{In}^{3-} defect does not carry a magnetic moment. The total energy of the spin-polarized state is 418 meV lower than that of nonspin-polarized state for the neutral indium vacancy. For V_{In}^{1-}, the preference of the spin-polarized state decreases to 206 meV, while there is a very small energy difference (49 meV) between the spin-polarized state and the nonspin-polarized state for the 2− charge state. Analysis of the spin density shows that the magnetic moment is mainly localized on the unpaired $2p$ electrons of the four nearest-neighboring N atoms. For the neutral In vacancy, each N atom of the three equivalent neighbors carries a magnetic moment of $0.65\mu_B$, and the remaining "apical" neighbor carries a magnetic moment of $0.67\mu_B$. With increasing occupation of the defect levels, the surrounding nitrogen atoms have a smaller average magnetic moment, $0.455\mu_B$/N for the 1− charge state and $0.25\mu_B$/N for the 2− charge state.

D. The V_N+N_{In} and V_N+V_{In} complexes

Very recently, Jones *et al.*[41] used high-energy particle irradiation to study the electron mobility in InN and suggested that in *n*-type material, the most stable defects are V_N, and the less stable defects are the relaxed V_{In}-like triply charged donor complexes, V_N+N_{In}. Soft x-ray adsorption spectroscopy studies support the above finding by indicating the presence of "trapped N_2 molecules." We are therefore motivated to investigate the defect complex V_N+N_{In} in both the "in-plane" (V_N and N_{In} both in the (0001) plane) and "out-of-plane" (V_N and N_{In} oriented in a direction parallel to the *c* axis) configurations. We find that the defect complexes are stable (as indicated by the large positive binding energies in Table II) and that the energy difference between these two configurations is only 3 meV in the neutral charge state, where the in-plane configuration is slightly favorable. We thus focus on this structure for further investigations. The neutral V_N+N_{In} defect complex introduces a doubly occupied singlet defect state and a singly occupied singlet defect state lying in the band gap, as well as several unoccupied defect states at higher energy. This complex can therefore act as a donor or an acceptor. We consider the charge states from 3+ to 3− and find that the 1− and 3− charge states are unstable (see Fig. 8); we thus do not consider further negative charge states. The calculated formation energy for this defect complex is slightly lower than the isolated indium vacancy but still too high for it to occur in appreciate concentrations in thermal equilibrium under either N-rich or In-rich conditions.

The average bond length between the antisite N_{In} and its three nearest-neighboring N atoms, forming a "N_4 molecule," slightly depends on the charge state: in the neutral state, it is 1.49 Å, and it increases to 1.50 Å in the 1+ charge state and decreases to 1.37 Å in the 3+ charge state. Adding electrons to the system results in a decrease in the N-N bond length, which is 1.44 Å in the 3− charge state.

It has been reported that the defect complex, V_N+V_{Ga} in GaN and V_N+V_{Al} in AlN, has a substantial binding energy and that its formation energy is lower than that of the isolated gallium vacancy under metal-rich conditions for *p*-type material.[42] It is interesting therefore to consider the interaction between the cation and anion vacancies (V_N+V_{In}) to see whether they prefer to bind together or be isolated in InN. We find that the cation-anion vacancy pair is stable (as indicated by the large positive binding energies in Table II). Configurations involving both in plane [V_N and V_{In} both in the (0001) plane] and out of plane (V_N and V_{In} oriented in a direction parallel to the *c* axis) have a very similar formation energy; e.g., for the neutral charge state the difference is only 3.5 meV. We consider the charge states only for the in-plane configuration since it is slightly lower in energy. The atomic structure is shown in Fig. 5(a). The neutral V_N+V_{In} defect complex introduces two singlet defect states above the VBM very close in energy as indicated by "D" in Fig. 5(b). The lower lying state is fully occupied with two electrons and the

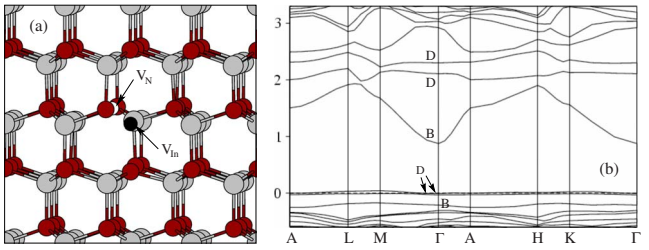

FIG. 5. (Color online) (a) Relaxed atomic geometry and (b) band structure of the vacancy complex V_N+V_{In} in the neutral charge state. Dark and light spheres represent N and In atoms, respectively, and small white and black spheres indicate the V_N and V_{In} sites, respectively, which are also indicated by arrows. Labels B and D in (b) represent bulk and defect states, respectively. The horizontally dotted line in (b) indicates the Fermi level.

other is unoccupied; thus, this complex may act as a donor or an acceptor. This complex also induces two unoccupied defect states above the CBM. We therefore consider the charge states $1\pm$ and $2\pm$ and find that the 2+ charge state is unstable. Similar to the V_N+V_{Ga} complex in GaN, the formation energy of V_N+V_{In} is lower than that of the isolated indium vacancy under In-rich conditions. However, the formation energies of the complex (V_N+V_{In}) are high, indicating that in thermal equilibrium this defect will not be present in significant concentrations. The V_N in the complex induces an outward relaxation for the positive charge state (1+) and inward relaxations in the neutral and negative charge states (see Table I). The breathing relaxation of the surrounding N atoms induced by V_{In} in the 1+ charge state is outward and becomes less so, or even slightly inward, with the increasing occupation.

E. Vacancy complexes

We now consider the possibility of indium vacancy complex formation. Here we investigate the atomic and electronic structures, as well as energetics, of up to three indium vacancies by performing an exhaustive search for the optimal spatial distribution (7 and 21 atomic configurations for 2 and 3 In vacancies, respectively). The energetics show that the indium vacancies prefer to cluster together, occupying nearest-neighbor [either in the (0001) plane or out-of-plane] sites.

For the neutral indium vacancy pair, the most favorable configuration is where the vacancies are located out of plane on the nearest-neighbor sites. Here the $V_{In}-V_{In}$ direction is not aligned parallel to the c axis but with an angle to it. The formation energy (per defect) for the neutral state is high, 5.95 eV under N-rich and 7.11 eV under In-rich conditions, and the binding energy indicates a strong attractive interaction (~1.8 eV per vacancy) as seen from Table II. After the relaxation [see Fig. 4(b)], a N-N bond forms with a distance of 1.23 Å, which is comparable to that of the N_2 dimer (1.10 Å). Due to the significant atomic relaxations, the $2V_{In}$ complex could be described as a N-spilt interstitial plus a mixed vacancy complex, V_N+2V_{In}. Once formed, the N-N bond is so strong that the total energy of this configuration is lower than that of the others by about 3.6 eV. The N-N bond

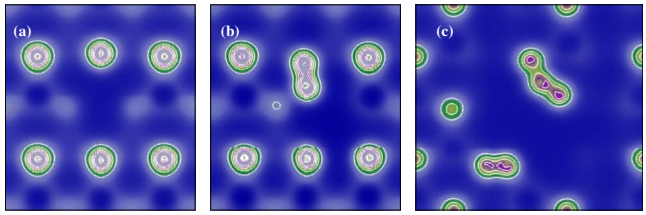

FIG. 6. (Color online) Contour plots of the electron charge density for (a) one, (b) two, and (c) three indium vacancies in InN in the neutral charge state. The lowest contour line value is at 0.0 e/Bohr^3, and the highest contour line has a value of 0.40 e/Bohr^3. Contour lines in between change successively by a factor of 0.08 e/Bohr^3.

can be clearly seen in the contour plot of the electron charge density in Fig. 6(b). The vacancy pair induces several defect states at the top of the valence band and in the conduction band, as indicated by the region between, and at, the arrows in the Fig. 7(a). There are two doubly occupied singlet states and the rest are unoccupied. We therefore consider charge states from 2+ to 6−. The stable charge states are 2+, 0, and 3−, and the others are unstable; thus, we do not consider further charge states. The binding energies for the stable charge states are listed in Table II. The binding energies of $2V_{In}$ in the neutral charge state are calculated with respect to the two neutral V_{In}, and for $2V_{In}^{3-}$ the binding energies (1.24 and 1.70 eV per vacancy) are computed with respect to V_{In}^{1-} and V_{In}^{2-}, and V_{In}^{0} and V_{In}^{3-}, respectively. For $2V_{In}^{4-}$, the binding

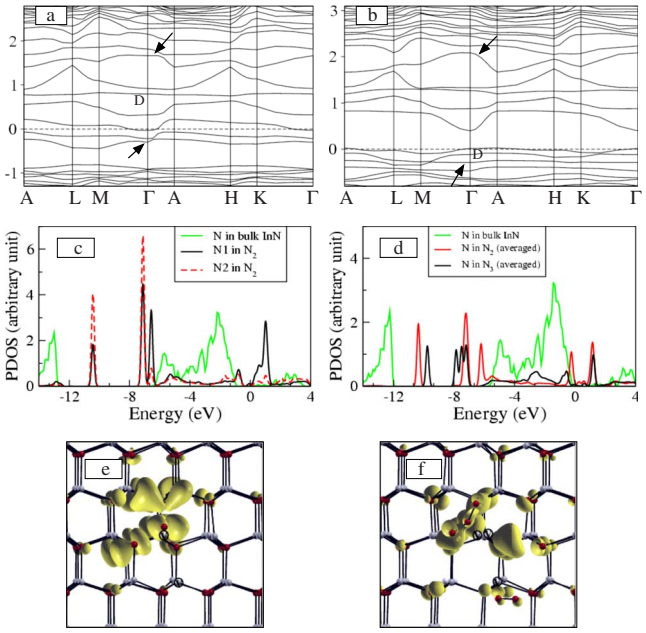

FIG. 7. (Color online) (a) and (b) Band structures, (c) and (d) partial density of states, (e) and (f) isosurface plots of the defect states [marked as D in (a) and (b)] of two and three indium vacancies in the neutral charge state, respectively. The arrows in (a) and (b) indicate the regions of the defect states; that is, all states between, and at, the arrows are defect induced states. The horizontally dotted lines indicate the Fermi levels. The 0.001 e/Bohr^3 isovalues are shown. Dark and light spheres represent N and In atoms, respectively, and open circles with "V" indicate the V_{In} sites.

energies, calculated with respect to V_{In}^{2-} and V_{In}^{2-}, and V_{In}^{1-} and V_{In}^{3-}, respectively, decrease to 0.41 and 0.65 eV per vacancy. The binding energies for the 5− and 6− charge states become negative, indicating a repulsive interaction between the two indium vacancies. In the 2+ charge state, the "nitrogen molecule" has a very similar N-N distance as for the neutral case. While in the 3− charge state, three N atoms around the vacancy pair form an independent N_3-like bonding arrangement with N-N bond lengths of 1.36 and 1.37 Å. For the higher negative charge states, the N_3-like configuration disappears, and only the "N_2-like molecule" exists.

For three In vacancies, the most favorable configuration is the one where one vacancy is located out of plane and the other two are in plane, again occupying nearest-neighbor sites. This preference can be seen from the large values (e.g. 3.28 eV/vacancy) for the neutral state of the binding energies in Table II. In the neutral charge state, the neighboring N atoms around the vacancies relax significantly to yield with an "N_2-like" geometry, and two other new N-N bonds are formed, resulting in an independent N_3-like configuration. The N-N bond length of "N_2" is 1.22 Å, and for the "N_3"-like configuration, the bond distances are 1.25 and 1.35 Å [see Fig. 4(c)], which are comparable to the N-N bond length (1.18 Å) of the gas phase azide (linear geometry) N_3 molecule.[43] The three In-vacancy complex, $3V_{In}$, induces many defect states, which are indicated in the region between, and at, the arrows in Fig. 7(b). In particular, the state at the Fermi level is occupied with one electron, and the three defect states below the Fermi level are each occupied with two electrons. We assign a state to be a defect state by plotting the square of the wave function and noting that it is weighted heavily on the defect, i.e., at, and between, the N atoms nearest to the vacancies. As an example, we show in Figs. 7(e) and 7(f) the defect states indicated by label "D" in Figs. 7(a) and 7(b) for the two- and three-indium vacancy clusters in the neutral charge state. We have carefully checked that all states lying between, and at, the arrows in Figs. 7(a) and 7(b) are indeed defect related states. We consider charge states from 3+ to 6−, and find that the 3+, 0, and 3− charge states are stable as shown in Fig. 8. The binding energies of all the negative charge states are larger than 0.6 eV, indicating attractive interactions between the vacancies. For instance, for $3V_{In}^{3-}$, the binding energies (2.45, 2.60, and 2.90 eV per vacancy) are computed with respect to three V_{In}^{1-}, $V_{In}^{0}+V_{In}^{1-}+V_{In}^{2-}$, and two V_{In}^{0} and V_{In}^{3-}, respectively. The N_2-like and "N_3-like" clusters remain for the various charge states, where the N-N bond lengths in both N_2 and N_3 increase slightly with increasing negative charge state. In the 3+ charge state, the N-N distance in N_2 is 1.19, and 1.23, and 1.33 Å in the N_3-like configuration. The respective values are 1.25, 1.30, and 1.39 Å in the 6− charge state. Figure 6(c) shows the contour plot of the electron charge density for $3V_{In}$ in the neutral charge state. The high density around the N_2- and N_3-like configurations can be clearly seen.

In Figs. 7(c) and 7(d), we show the density of states for the two- and three-indium vacancy clusters, respectively. It is evident that all the N atoms in the "molecules" induce additional peaks both in the valence band and in the conduction band, which are again quite different to the bulk (In-bonded) N atoms. Such In-vacancy complex induced states may be a "fingerprint" for identifying the existence of these structures experimentally.

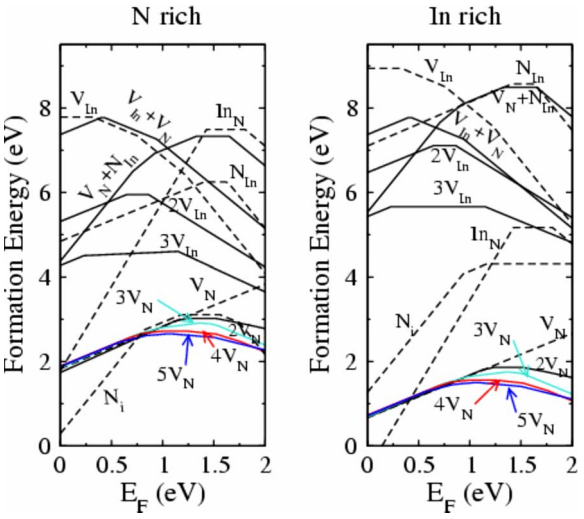

FIG. 8. (Color online) Formation energies as a function of the Fermi level for anion and cation vacancies (per nitrogen or indium vacancy), antisites, N interstitial, and complexes in wurtzite InN under N-rich (left) and In-rich (right) conditions. The zero of the Fermi level corresponds to the top of the valence-band maximum. The dashed lines represent the isolated point defects, and the solid lines correspond to defect complexes. Results for the nV_N complexes are from Ref. 27.

In our previous paper,[27] we found that the isolated nitrogen vacancy acts as a single or triple donor in *p*-type material, where for In-rich conditions it is the lowest-energy native defect. We also reported that nitrogen vacancies prefer to be situated close to one another forming "vacancy complexes or clusters" resulting in local indium-rich regions with metalliclike bonding. We include the associated formation energies from that study for the nitrogen vacancy and vacancy complexes in Fig. 8.

Figure 8 summarizes formation energies of all the defects considered as a function of the Fermi level, E_F, under N- and In-rich conditions. The formation energies for vacancy clusters are given per vacancy to highlight the preference for clustering. We only show the segments corresponding to the lowest-energy charge states, and the slopes of the lines correspond to the charge state (divided by the number of vacancies for the vacancy defect complexes). Under In-rich and *p*-type conditions, the indium antisite in the 4+ charge state has the lowest formation energy. The next most favorable defect is the single nitrogen vacancy in the 1+ charge state, but the positively charged nitrogen vacancy clusters are only marginally less favorable (practically degenerate). For more *n*-type material, the neutral and negatively charged nitrogen vacancy clusters become favorable (per vacancy). For example, the formation energy of the four nitrogen vacancy clusters ($4V_N$) is 1.56 eV/vacancy, that is, 6.24 eV for $4V_N$ complex. This is clearly a high formation energy indicating that the concentration of such structure under thermal equilibrium will be low. It is possible, however, that these structures may form under nonequilibrium growth conditions. For N-rich conditions, the nitrogen split interstitial has the lowest

formation energy and thus could be a dominant defect, contributing to the high background electron conductivity, along with the nitrogen vacancy and the indium antisite under more In-rich conditions.

IV. DISCUSSION

We will now compare our results with the available experimental observations. For N-rich molecular-beam-epitaxy (MBE)-grown films, the UV-Raman spectrum shows evidence of excess nitrogen, and the nitrogen antisite is implicated to be one of the favorable defects for excess nitrogen in InN.[21] Other possibilities, however, such as molecular nitrogen or di-nitrogen interstitials cannot be excluded. Using swift ions, Timmers *et al.*[44] suggested that InN contains N atoms or molecules interstitially. Under N-rich conditions, the formation of In vacancies, N_2, and the antisite N_{In} have been reported; and under In-rich conditions, the formation of N vacancies and In_N have been observed by energy-dispersive x-ray analysis for InN films grown at 300–550 °C.[23] Jones *et al.*[41] suggested that in *n*-type material, nitrogen vacancies and the V_{In}-like triply charged donor complexes, V_N+N_{In}, are the favorable defects. According to our calculations, the nitrogen split interstitial is the most favorable defect under N-rich conditions which results in an N_2-like bonding configuration. We note furthermore that the N_i defect could also serve as a potential source of the *n*-type conductivity. We suggest that the nitrogen split interstitial could be the defect which results in the N-N bonding as measured by the UV-Raman system,[21] N_2 dimer[23] or interstitial N atoms or molecules.[44] The calculated formation energy for the nitrogen antisite, which could also be described as the complex (V_{In}+N split interstitial) and the defect complex V_N+N_{In} in *n*-type material, is too high for it to occur in appreciate concentrations in thermal equilibrium under either N-rich or In-rich conditions. The In-vacancy clusters could exist under N-rich condition, giving rise to nitrogen-molecular-like bonding configurations. Under In-rich conditions and in *p*-type material, In_N^{4+} has the lowest formation energy, which is consistent with energy-dispersive x-ray analysis of Ref. 23. Nitrogen vacancy clusters are favored under N- and In-rich conditions for *n*-type material.[45] The metalliclike In inclusions reported by Davydov *et al.*[46] may be due to N-vacancy clusters.

Using both positron lifetime and Doppler broadening measurements, positron annihilation spectroscopy in the MBE-grown InN layers showed a clear sign of In vacancies,[47] and a high vacancy concentration, indicating that the N-rich stoichiometry of the material could be related to the presence of indium vacancy clusters. The formation energy of the In-vacancy pair is high; however, on considering three vacancy clusters, the formation energy decreases by 1.5 eV/vacancy. We may expect a decreasing formation energy with additional indium vacancies. At what size vacancy cluster the formation energy (per vacancy) will saturate, however, is unclear. Very recently, the cation vacancy clusters consisting of four to five missing atoms in SiC have been identified by positron lifetime spectroscopy.[48] Also oxygen vacancy clustering was also reported in $SrTiO_3$ by means of the transmission electron microscopy.[49]

V. CONCLUSION

We performed first-principles calculations to investigate the atomic and electronic structures of vacancy defects and complexes, as well as antisites and the nitrogen interstitial in wurtzite InN. We found that the nitrogen antisite, nitrogen interstitial, and indium vacancy clusters give rise to the formation of N-N bonded molecularlike configurations. The indium antisite and nitrogen vacancy clusters result in local In-rich regions. Under N-rich conditions, the nitrogen interstitial is a triple donor and has the lowest formation energy in more *p*-type material; and under In-rich conditions, the indium antisite in 4+ charge state has the lowest formation energy in *p*-type material. The nitrogen vacancy complexes in the neutral and negative charge states become more favorable for more *n*-type material. Our results provide theoretical evidence for the above-mentioned experimental observation[21,23] of nitrogen molecules, antisites, and interstitials. The indium vacancy clusters (up to three vacancies) have rather higher formation energies; however, the formation of larger indium vacancy clusters cannot be excluded since the formation energy decreases (per vacancy) significantly with increasing number of vacancies in the cluster. Further theoretical and experimental studies are necessary to investigate this possibility.

ACKNOWLEDGMENTS

The authors gratefully acknowledge financial support from the Australian Research Council (ARC) and supercomputing resources from the Australian Partnership for Advanced Computing (APAC) National Facility and Australian Center for Advanced Computing and Communications (AC^3).

[1] I. Vurgaftman, J. R. Meyer, N. Tansu, and L. J. Mawst, Appl. Phys. Lett. **83**, 3742 (2003).
[2] T. Matsuoka, H. Okamoto, H. Takahata, T. Mitate, S. Mizuno, Y. Uchiyama, and T. Makimoto, J. Cryst. Growth **269**, 139 (2004).
[3] S. K. O'Leary, B. E. Foutz, M. S. Shur, and L. F. Eastman, Appl. Phys. Lett. **88**, 152113 (2006).
[4] R. Hui, S. Taherlon, Y. Wan, J. X. Lin, J. Y. Lin, and H. X. Jiang, Appl. Phys. Lett. **34**, L1332 (1995).
[5] J. Wu, W. Walukiewicz, K. M. Yu, W. Shan, J. W. Ager III, E. E. Haller, H. Lu, W. J. Schaff, W. K. Metzger, and S. Kurtz, J. Appl. Phys. **94**, 6477 (2003).
[6] E. Starikov, P. Shiktorov, V. Gruzinskis, L. Reggiani, L. Varani, J. C. Vaissiére, and H. Zhao, Physica B **314**, 171 (2002); Mater. Sci. Forum **384–385**, 205 (2002).
[7] W. Walukiewicz, J. W. Ager III, K. M. Yu, Z. Liliental-Weber, J. Wu, S. X. Li, R. E. Jones, and J. D. Denlinger, J. Phys. D **39**,

R83 (2006).
[8] K. Osamura, K. Nakajima, Y. Murakami, P. H. Shingu, and A. Ohtsuki, Solid State Commun. **11**, 617 (1972).
[9] T. L. Tansley and C. P. Foley, J. Appl. Phys. **59**, 3241 (1986).
[10] G. D. Chern, E. D. Readinger, H. Shen, M. Wraback, C. S. Gallinat, G. Koblmüller, and J. S. Speck, Appl. Phys. Lett. **89**, 141115 (2006).
[11] V. Y. Davydov, A. A. Klochikhin, R. P. Seisyan, V. V. Emtsev, S. V. Ivanov, F. Bechstedt, J. Furthmüller, H. Harima, V. Mudryi, J. Aderhold, O. Semchinova, and J. Graul, Phys. Status Solidi B **229**, R1 (2002).
[12] J. Wu, W. Walukiewicz, K. M. Yu, J. W. Ager III, E. E. Haller, H. Lu, W. J. Schaff, Y. Saito, and Y. Nanishi, Appl. Phys. Lett. **80**, 3967 (2002).
[13] M. Usuda, N. Hamada, K. Shiraishi, and A. Oshiyama, Jpn. J. Appl. Phys. **43**, L407 (2004).
[14] A. Sher, M. van Schilfgaarde, M. A. Berding, S. Krishnamurthy and A. B. Chen, MRS Internet J. Nitride Semicond. Res. **4S1**, G5.1 (1999).
[15] F. Bechstedt and J. Furthmüller, J. Cryst. Growth **246**, 315 (2002).
[16] J. Furthmüller, P. H. Hahn, F. Fuchs, and F. Bechstedt, Phys. Rev. B **72**, 205106 (2005).
[17] P. Rinke, M. Scheffler, A. Qteish, M. Winkelnkemper, D. Bimberg, and J. Neugebauer, Appl. Phys. Lett. **89**, 161919 (2006).
[18] T. V. Shubina, S. V. Ivanov, V. N. Jmerik, D. D. Solnyshkov, V. A. Vekshin, P. S. Kopev, A. Vasson, J. Leymarie, A. Kavokin, H. Amano, K. Shimono, A. Kasic, and B. Monemar, Phys. Rev. Lett. **92**, 117407 (2004).
[19] T. Matsuoka, H. Okamoto, M. Nakao, H. Harima, and E. Kurimoto, Appl. Phys. Lett. **81**, 1246 (2002).
[20] M. Yoshimoto, H. Yamamoto, W. Huang, H. Harima, J. Saraie, A. Chayahara, and Y. Horino, Appl. Phys. Lett. **83**, 3480 (2003).
[21] K. S. A. Butcher, M. Wintrebert-Fouquet, P. P.-T. Chen, T. L. Tansley, H. Dou, M. Kuball, K. E. Prince, and J. E. Bradby, J. Appl. Phys. **95**, 6124 (2004).
[22] P. Specht, R. Armitage, J. Ho, E. Gunawan, Q. Yang, X. Xu, C. Kisielowski, and E. R. Weber, J. Cryst. Growth **269**, 111 (2004).
[23] T. V. Shubina, S. V. Ivanov, V. N. Jmerik, M. M. Glazov, A. P. Kalvarskii, M. G. Tkachman, A. Vasson, J. Leymarie, A. Kavokin, H. Amano, I. Akasaki, K. S. A. Butcher, Q. Guo, B. Monemar, and P. S. Kopev, Phys. Status Solidi A **202**, 377 (2005).
[24] C. Stampfl, C. G. Van de Walle, D. Vogel, P. Krüger, and J. Pollmann, Phys. Rev. B **61**, R7846 (2000).
[25] T. L. Tansley and R. J. Egan, Phys. Rev. B **45**, 10942 (1992); *Wide Band-Gap Semiconductors*, MRS Symposia Proceedings No. 242, (Materials Research Society, Pittsburgh, 1992), p. 395.
[26] D. W. Jenkins and J. D. Dow, Phys. Rev. B **39**, 3317 (1989).
[27] X. M. Duan and C. Stampfl,Phys. Rev. B **77**, 115207 (2008).
[28] S. Baroni, A. Dal Corso, S. de Gironcoli, and P. Giannozzi, http://www.pwscf.org
[29] S. G. Louie, S. Froyen, and M. L. Cohen, Phys. Rev. B **26**, 1738 (1982).
[30] C. G. Van de Walle and J. Neugebauer, J. Appl. Phys. **95**, 3851 (2004).
[31] *Properties of Group-III Nitrides*, EMIS Datareviews Series, edited by J. H. Edgar (IEE, London, 1994).
[32] Here we used the DMOL (Ref. 3) code described in B. Delley, J. Chem. Phys. **113**, 7756 (2000); **92**, 508 (1990). The wave functions are expanded in terms of a double-numerical quality localized basis set with a cutoff radius of 11 Bohr. Brillouin zones are performed using a $(6\times6\times4)$ Monkhorst-Pack grid.
[33] C. Kittel, *Introduction to Solid State Physics* (Wiley, New York, 1986).
[34] R. W. G. Wyckoff, *Crystal Structures* (Wiley, New York, 1963), Vol. I.
[35] CRC Handbook of Chemistry and Physics, 77th ed., edited by D. R. Lide (CRC, Boca Raton, FL, 1997).
[36] M. Fuchs, J. L. F. Da Silva, C. Stampfl, J. Neugebauer, and M. Scheffler, Phys. Rev. B **65**, 245212 (2002).
[37] C. Stampfl and C. G. Van de Walle, Phys. Rev. B **65**, 155212 (2002).
[38] Sukit Limpijumnong and C. G. Van de Walle, Phys. Rev. B **69**, 035207 (2004).
[39] A. Savin, O. Jepsen, J. Flad, O. K. Andersen, H. Preuss, and H. G. Von Schneiring, Angew. Chem., Int. Ed. Engl. **31**, 187 (1992).
[40] R. Q. Wu, G. W. Peng, L. Liu, Y. P. Feng, Z. G. Huang, and Q. Y. Wu, Appl. Phys. Lett. **89**, 142501 (2006).
[41] R. E. Jones, H. C. M. van Genuchten, S. X. Li, L. Hsu, K. M. Yu, W. Walukiewicz, J. W. Ager III, E. E. Haller, H. Lu, and W. J. Schaff, *GaN, AIN, InN, and Related Materials*, MRS Symposia Proceedings No. 892, (Materials Research Society, Pittsburgh, 2006), p. FF06.
[42] M. G. Ganchenkova and R. M. Nieminen, Phys. Rev. Lett. **96**, 196402 (2006).
[43] C. R. Brazier, P. F. Bernath, J. B. Burkholder, and C. J. Howard, J. Chem. Phys. **89**, 1762 (1988).
[44] H. Timmers, K. S. A. Butcher, S. K. Shrestha, P. P.-T. Chen, M. Wintrebert-Fouquet, and R. Dograhi, J. Cryst. Growth **288**, 236 (2006).
[45] Using the nudged elastic band method and the 96-atom supercell, we obtain a migration barrier (along the c axis) of 3.2 eV for V_N in the 1+ charge state, and for V_{In} in the 3− charge state, we obtained 1.6 eV (also along the c axis). These values can be compared with those of 4.3 and 1.9 eV for V_N^+ and V_{Ga}^{3-} in GaN (Ref. 38). Our smaller values could be related to the larger lattice constant of InN compared to GaN, and hence the atoms have more space to relax as the vacancy diffuses. Following the approach of Ref. 38, a migration energy of 3.2 and 1.6 eV would imply that diffusion due to nitrogen and indium vacancies could occur at temperatures around 1100 and 700 K, respectively.
[46] V. Y. Davydov, A. A. Klochikhin, V. V. Emtsev, S. V. Ivanov, V. V. Vekshin, F. Bechstedt, J. Furthmuller, H. Harima, A. V. Mudryi, A. Hashimoto, A. Yamamoto, J. Aderhold, J. Graul, and E. F. Haller, Phys. Status Solidi B **230**, R4 (2002); **240**, 425 (2003).
[47] A. Laakso, J. Oila, A. Kemppinen, K. Saarinen, W. Egger, L. Liszkay, P. Sperr, H. Lu, and W. J. Schaff, J. Cryst. Growth **269**, 41 (2004).
[48] R. Aavikko, K. Saarinen, F. Tuomisto, B. Magnusson, N. T. Son, and E. Janzen, Phys. Rev. B **75**, 085208 (2007).
[49] D. D. Cuong, B. Lee, K. M. Choi, H. S. Ahn, S. Han, and J. Lee, Phys. Rev. Lett. **98**, 115503 (2007).